

Easy attention: A simple attention mechanism for temporal predictions with transformers

Marcial Sanchis-Agudo¹, Yuning Wang¹, Roger Arnau²,

Luca Guastoni¹, Jasmin Lim³, Karthik Duraisamy^{3,4}, Ricardo Vinuesa¹

1: *FLOW, Engineering Mechanics, KTH Royal Institute of Technology, SE-100 44 Stockholm, Sweden.*

2: *Instituto Universitario de Matemática Pura y Aplicada,*

Universitat Politècnica de València. Camino de Vera s/n, 46022 València, Spain.

3: *Department of Aerospace Engineering, University of Michigan, Ann Arbor, USA.*

4: *Michigan Institute for Computational Discovery & Engineering (MICDE), University of Michigan, Ann Arbor, USA.*

To improve the robustness of transformer neural networks used for temporal-dynamics prediction of chaotic systems, we propose a novel attention mechanism called easy attention which we demonstrate in time-series reconstruction and prediction. While the standard self attention only makes use of the inner product of queries and keys, it is demonstrated that the keys, queries and softmax are not necessary for obtaining the attention score required to capture long-term dependencies in temporal sequences. Through the singular-value decomposition (SVD) on the softmax attention score, we further observe that self attention compresses the contributions from both queries and keys in the space spanned by the attention score. Therefore, our proposed easy-attention method directly treats the attention scores as learnable parameters. This approach produces excellent results when reconstructing and predicting the temporal dynamics of chaotic systems exhibiting more robustness and less complexity than self attention or the widely-used long short-term memory (LSTM) network. We show the improved performance of the easy-attention method in the Lorenz system, a turbulence shear flow and a model of a nuclear reactor.

Keywords: Machine Learning, Transformer, Self Attention, Koopman Operator, Chaotic System.

Introduction

Dynamical systems are mathematical models used to describe the evolution of complex phenomena over time. These systems are prevalent in various fields, including physics and engineering. A dynamical system consists of variables that change over time, and their interactions are governed by differential equations. The behavior of such systems can range from simple and predictable to highly complex and chaotic. Furthermore, chaotic systems are characterized by their sensitivity to perturbations of the initial conditions, leading to unpredictability and complex dynamics. The prediction of chaotic dynamical systems stands as a relevant and challenging area of study. Accurate forecasting of such systems holds significant importance in diverse scientific and engineering disciplines, including weather forecasting, ecological modeling, financial analysis, and control of complex physical processes.

Dynamical-system models leveraging the concept of time delays [1–4] have been applied for temporal-dynamics prediction. These models also leverage decomposition to obtain a reduced-order representation of the system. For instance, proper-orthogonal decomposition [5] provides a set of deterministic spatial functions with corresponding time coefficients. The decomposition can also be performed in the spectral domain [6]. Another widely used method in different scientific fields is the dynamic-mode decomposition (DMD) [7, 8] which captures intricate temporal patterns and can reveal underlying modes of motion. DMD represents a numerical approach to the approximation of the Koopman operator [2, 9–11]. Koopman-based frameworks have achieved promising results in the prediction of temporal dynamics of high-dimensional chaotic systems [12–16]. In the context of time-series analysis, the well-known family of auto-regressive and moving-average (ARMA) models is used for forecasting dynamical systems [17]. These methods focus on stochastic problems and they yield interpretable models [4]. Deep neural networks (DNNs), as a branch of machine-learning (ML) approaches, have demonstrated remarkable success in temporal-dynamics prediction, offering advantages of flexibility and adaptability. The family of recurrent neural networks (RNNs) [18] has been the dominant method for temporal-dynamics prediction for many years, enabling the model to capture temporal dependencies in the time series. Among RNNs, the long short-term memory (LSTM) networks [19] overcome the training problems related to vanishing gradients and this enables modelling long-term dependencies. Herefore, LSTM networks are effective ML models for temporal predictions of complex dynamical systems [16, 20, 21]. Besides RNNs, the temporal convolutional networks (TCNs) [22], which employ one-dimensional convolutions for multi-variable time-series prediction [23, 24], have shown promising performance on temporal-dynamics prediction [25].

In recent years, transformer neural networks [26] have revolutionized the field of ML, demonstrating remarkable capabilities in natural-language processing (NLP) [27] and computer vision [28], but also fluid mechanics [29]. Thanks to their matrix-multiplication-based attention mechanism [26], transformers have shown the capability to identify and predict the temporal dynamics of chaotic systems by capturing long-term dependencies in the data [25, 30, 31]. This promising performance has motivated several studies focused on improving the attention mechanism of transformer

models used for physical modeling [32, 33]. Additionally, in the context of reducing complexity in NLP, more studies on improving attention mechanism, in particular self-attention, have emerged [34–36], and they have reported promising results while reducing the computational cost. Note that all the mentioned improvements on self-attention follow the idea of the retrieval process which comprises queries, keys and values. However, in the present study, inspired by work done on Koopman operators [13–16], we propose a new attention mechanism denoted by easy attention, which use neither the softmax [32, 35] nor the linear projections of queries and keys; this has the goal of reducing the complexity of the model and improving its interpretability. Our objective is to predict the temporal evolution of dynamical systems. Typically, self-attention is computed for every input; however, this choice can be less effective in chaotic systems as the input can vary arbitrarily, while keeping the same underlying system dynamics. Conservative attractors remain invariant under small perturbations as proposed by Kolmogorov–Arnold–Moser (KAM) Theory [37]. Based on this intuition, we propose an easy-attention formulation that is optimized during training and it is not input-dependent at inference time. Doing so, we learn an importance score for the input variables that encodes the system dynamics rather than the instantaneous attention of the input values. This approach provides significant performance improvements in the prediction of the trajectories of chaotic systems, as it fully exploits the spatial periodicity that is naturally present in most chaotic systems, assuming an underlying constant pattern over time, the invariant set.

Interpretation of attention mechanism

In this section, we provide a motivating example for simplifying the self-attention mechanism and propose the easy-attention technique described in the Methods section. We start with a reconstruction task of a simple wave function, using the self-attention module. Based on the data, we investigate the eigenspace given by the self-attention mechanism, and analyze the main limitation of this mechanism. Subsequently, we discuss how to address such limitation using the easy attention method and we compare the reconstruction results.

Harmonic functions are often used in the study of temporal signals, therefore, in our example, we consider three sine waves with the same frequency but different phase shifts, expressed as:

$$y_i(t_j) = \sin\left(t_j \frac{\pi}{2} + i - 1\right); \quad t_j \in \mathbb{N}, \quad j, i \in \mathbb{Z}, \quad (1)$$

where t is time spanning the range $[0, 3N]$ and each y_i a trajectory. A satisfactory performance of the different attention mechanisms for this case is a prerequisite to attempt the prediction of more challenging problems. Here our focus is on identification and reconstruction of the wave motion and we assess the results obtained just with the attention module, without any extra hidden layers and activation functions. For this case, each sample consists of the three sine waves with different phase shifts at 3 consecutive time instants, $\mathbf{y}_i = \{y_i(t_{3p} - k\Delta t)\}_{k=0}^2$, where $\Delta t = 1$. Interpreting \mathbf{y}_i as a column vector, we can write the input matrix for the attention mechanism as $\mathbf{Y} = \text{concat}\{\mathbf{y}_i\}_{i=1}^3$, where concat refers to concatenation, as represented in Eq. (2). Here we refer to p as the current sample in the batch and n as the time delay.

$$\mathbf{Y} = \begin{bmatrix} y_1(t_{3p} - 2) & y_2(t_{3p} - 2) & y_3(t_{3p} - 2) \\ y_1(t_{3p} - 1) & y_2(t_{3p} - 1) & y_3(t_{3p} - 1) \\ y_1(t_{3p}) & y_2(t_{3p}) & y_3(t_{3p}) \end{bmatrix}. \quad (2)$$

We train the model to predict the value of the sine waves at the next three time steps, *i.e.* $\{\mathbf{y}(t_{3p} + k\Delta t)\}_{k=1}^3$. In order to perform the training, we adopt stochastic gradient descent (SGD) with momentum of 0.98 as optimiser, and the learning rate is set to 10^{-3} . The mean-squared error (MSE) is employed as loss function:

$$\text{MSE} = \left\langle \sum_{k=1}^3 \sum_{i=1}^3 (y_i(t_{3p} + k\Delta t) - \hat{y}_i(t_{3p} + k\Delta t))^2 \right\rangle_{p \in \text{batch}}, \quad \text{batch} \subseteq [0, N] \quad (3)$$

where y_i and \hat{y}_i indicate the ground truth and the corresponding prediction, respectively. The model is trained for 1,000 epochs, $N = 1 \times 10^3$ and batch size of 8. In order to compute the self attention, we need to construct the query, key and value matrices as described in Ref. [26], specifically $\mathbf{W}_Q, \mathbf{W}_K, \mathbf{W}_V \in \mathbb{R}^{3 \times 3}$:

$$\mathbf{Q}(\mathbf{y}_i) = \mathbf{W}_Q^T \mathbf{y}_i, \quad \mathbf{K}(\mathbf{y}_i) = \mathbf{W}_K^T \mathbf{y}_i, \quad \mathbf{V}(\mathbf{y}_i) = \mathbf{W}_V^T \mathbf{y}_i. \quad (4)$$

Note that the query and key matrices are used to compute the dot product $\langle \mathbf{Q}(\mathbf{y}_i), \mathbf{K}(\mathbf{y}_j) \rangle$ and the attention scores $\alpha_{ij} = \text{softmax}_j(\langle \mathbf{Q}(\mathbf{y}_i), \mathbf{K}(\mathbf{y}_j) \rangle / \sqrt{k})$, where k is the well known dmodel size for transformers or latent dimension. Since the trace of the operator is invariant to cyclic permutations of its argument, we can write:

$$\langle \mathbf{Q}(\mathbf{y}_i), \mathbf{K}(\mathbf{y}_j) \rangle = \langle \mathbf{K}(\mathbf{y}_j), \mathbf{Q}(\mathbf{y}_i) \rangle = \text{Tr}(\mathbf{W}_Q \mathbf{W}_K^T \mathbf{y}_j \mathbf{y}_i^T). \quad (5)$$

This enables identifying two matrices: $\mathbf{W}_Q \mathbf{W}_K^T$ and $\mathbf{y}_j \mathbf{y}_i^T$. We will refer to α_{ij} as the transformed covariance factor given that $\alpha = \mathbf{C} \iff \mathbf{W}_Q \mathbf{W}_K^T = \mathbb{I}$, where \mathbb{I} is the identity matrix, $\mathbf{C} = \mathbf{Y}^T \mathbf{Y}$ is the covariance matrix of the input matrix \mathbf{Y} and $C_{i,j} = \text{Tr}(\mathbf{y}_j \mathbf{y}_i^T)$ the covariance factor; note that $\mathbf{y}_j \mathbf{y}_i^T$ is the covariance factor matrix. Due to the rank-1 nature of the covariance factor matrix, performing the eigen-decomposition of the latter would not allow us to extract any relevant information. In order to address this issue, we apply singular-value decomposition (SVD) [38] to the matrix product $\mathbf{W}_Q \mathbf{W}_K^T \mathbf{y}_j \mathbf{y}_i^T$ in order to gain insight into its structure.

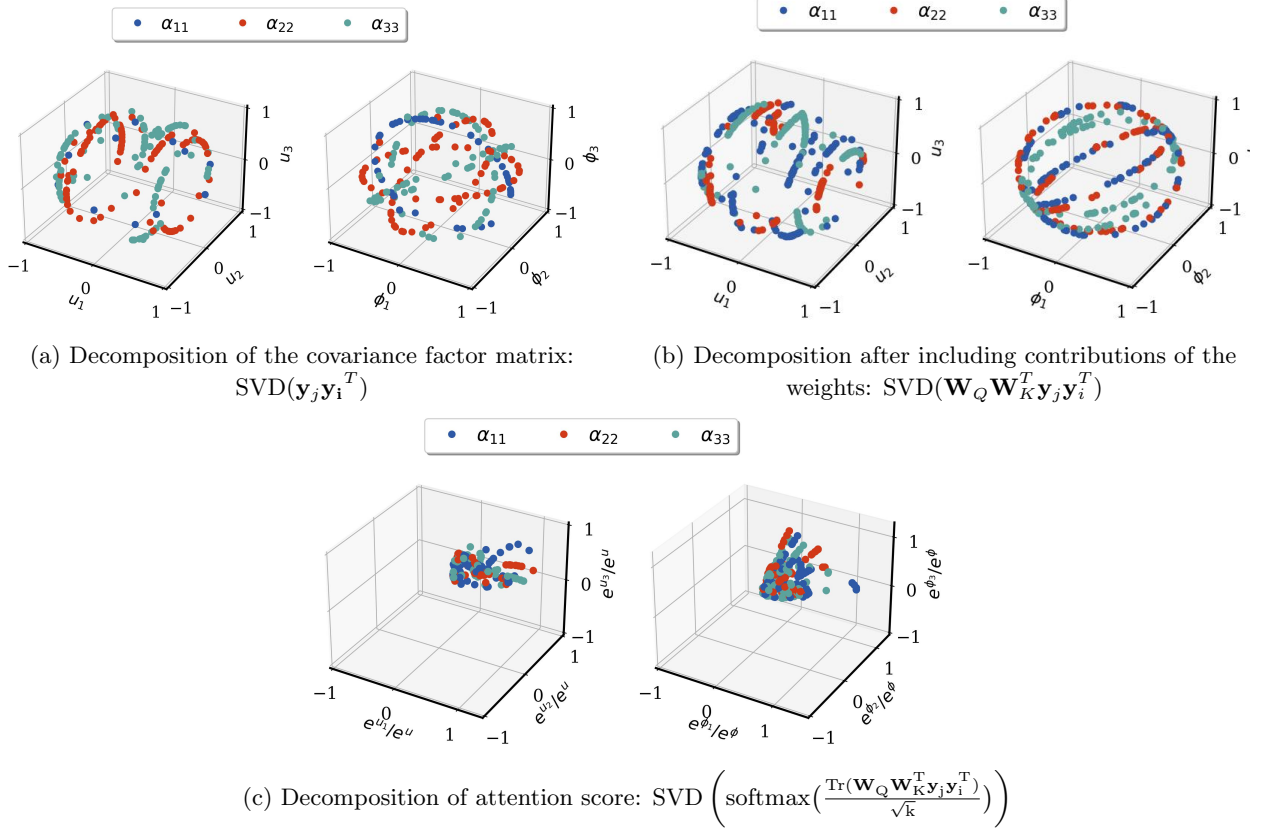


FIG. 1: **Three-dimensional scatter plots of left and right singular vectors (u_i and ϕ_i) of diagonal elements in the transformed covariance matrix α of the inputs.** Singular Value Decomposition of the (a) covariance factor matrix, (b) transformed covariance factor matrix and (c) attention score. The diagonal elements are denoted by black (α_{11}), red (α_{22}) and cyan (α_{33}), respectively.

The SVD of the transformed covariance factor matrix given by $\mathbf{y}_j \mathbf{y}_i^T$ as well as the product of the query and key matrices used to later compute the attention scores, together with the corresponding scores in α are shown in Fig. 1. Note that we only show the main diagonal elements of the α matrix as these are the main contributors when computing the attention score. From the transformed covariance factor matrix, one can observe that the spanned space by the left singular vectors, \mathbf{u} , exhibits an approximately cylindrical shape. However, the right singular vectors ϕ exhibit a shape closer to that of a sphere. These shapes are connected within the unit circle, which is used to study unique sinusoidal functions. When analyzing multiple waves with different phase shifts, given orthogonal phase shifts, the unit circle is expected to grow in dimensions as the transformed covariance factor matrix between input vectors increases. It can be claimed that as $r \rightarrow \infty$ for $\mathbf{Y} \in \mathbb{R}^{3 \times r}$, the sphere will become denser, creating a fully compact surface if and only if the new waves in Eq. (2) are linearly independent with the rest of input columns. The eigenspaces for queries and keys, shown in Fig. 1(b), are observed to be fixed by rotations and translations of $\mathbf{W}_Q \mathbf{W}_K^T$. These orbits constitute the subspace of the real domain, where the inner product exists. However, after the space compression forced by the trace and softmax, this subdomain is reduced to a scalar, which is shown in Fig. 1(c) as a non-trivial space compression. One can interpret α as the transformed covariance matrix between inputs of the transformer, such that $\alpha_{i,j} \in [0, 1], \forall i, j$. In fact, the softmax is a probability distribution over three different possible trajectories, each trajectory being an input vector. For instance, the second element in the first row of α is expressed as:

$$\alpha_{1,2} = \frac{\exp\left(\frac{\text{Tr}(\mathbf{y}_2 \mathbf{y}_1^T \mathbf{W}_Q \mathbf{W}_K^T)}{\sqrt{k}}\right)}{\sum_{j=1}^3 \exp\left(\frac{\text{Tr}(\mathbf{y}_j \mathbf{y}_1^T \mathbf{W}_Q \mathbf{W}_K^T)}{\sqrt{k}}\right)}. \quad (6)$$

In Eq. (6), it can be observed that the numerator fulfills $\exp\left(\frac{\text{Tr}(\mathbf{W}_Q \mathbf{W}_K^T \mathbf{y}_2 \mathbf{y}_1^T)}{\sqrt{k}}\right) = \exp\left(\frac{\sum_{i=1}^3 \lambda_i}{\sqrt{k}}\right)$, where λ_i represent the eigenvalues of the matrix, and this is, after normalization, the attention factor between \mathbf{y}_1 and \mathbf{y}_2 : $\alpha_{1,2}$. The latter behaves like a probability distribution: when we combine all possible trajectories spanned by all possible $x_j = \mathbf{V}(\mathbf{y}_j)$ with their respective attention factors, we obtain the expected trajectory as a reconstruction for the next time instances of the time series \mathbf{y}_1 , expressed as $\hat{\mathbf{y}}_1$. Therefore, for a fixed i and $X_i = \{x_1, x_2, x_3\}$ with probabilities $p_j = \alpha_{i,j}$:

$$\mathbb{E}(X_i) = \sum_{j=1}^3 p_j x_j = \sum_{j=1}^3 \alpha_{i,j} \mathbf{W}_V \mathbf{y}_j = \hat{\mathbf{y}}_i. \quad (7)$$

When computing the trace we compress all spatio-temporal dependencies. In a continuous sense, this can be interpreted as a weighted integration over the past time. In conclusion, the α matrix highlights the temporal dependencies between time instances, while \mathbf{W}_V includes the dependence of spatial inputs. In this example, due to the independence between wave phases, \mathbf{W}_V should become a near-diagonal matrix. It is not possible to make any strong claim regarding α , as the key of our approach is to relax any assumption on temporal dependencies and learn a hidden optimal temporal basis, *i.e.* local minimum.

It is important to recognize the difference between language (for which the self-attention framework was mainly developed) and physical problems. When analyzing text, the attention matrix is mostly diagonal, nearly a bijective mapping, as for each word that we input there exists a (near) one-to-one relationship with another word in the ground truth. However, for physical problems this behavior cannot be assumed and it becomes obvious during the training phase.

Based on the discussion above, the nature of the trace eliminates all backwards traceability of the information, decreasing the relevance of the exact value of each matrix element. Therefore, it is reasonable to directly learn the exact α value instead of learning the query and key matrices. Here, we propose removing the \mathbf{W}_K , \mathbf{W}_Q and softmax from the self attention, which (assuming square matrices \mathbf{W}_K and \mathbf{W}_Q after embedding into the latent dimension k) reduces the computational complexity of the problem from $4n_i^2$ to $2n_i^2$, where n_i is the size of the input vectors, $\mathbf{y}_i(t)$. Note that other kinds of attention methods exist besides the dot-product-based one shown in Eq. (6). This is the case of the neural machine translation version presented in Ref. [39], in which the attention scores are computed directly as the output of a recurrent neural network the inputs of which are the past observations. However, in easy attention, those scores are learned and then fixed, so they are independent on the past observations, allowing for a constant-operator interpretation of the model as in Koopman theory and Hamiltonian mechanics.

At this stage, we employ the easy-attention module using an input of the same size as that of the self attention, and the same training setup for sinusoidal-waves reconstruction. We evaluate the reconstruction accuracy by the relative l_2 -norm error defined as:

$$\varepsilon = \frac{\|S - \tilde{S}\|_2}{\|S\|_2}, \quad (8)$$

where S is the ground-truth sequence and \tilde{S} is the prediction obtained by the attention module. In the Supplementary Material we show details regarding l_2 -norm errors, computation time for training (t_c) and number of floating-point operations (N_f) of the employed easy-attention and self-attention modules. The results indicate that easy attention reduces the complexity of self attention by 45%, saves computation time by 15% and outperforms the self-attention, with an error of 0.0018% compared with the 10% given by the latter.

Temporal-dynamics predictions of chaotic systems using a transformer network with easy attention

In the following section we will use a modified transformer encoder with easy attention in order to conduct a systematic study regarding the performance of the latter against other state-of-the-art deep-learning models. In particular, we first study the Lorenz system (a three-dimensional canonical chaotic system), secondly the Moehlis model [40] for wall-bounded turbulence (which is a system comprising nine ordinary differential equations) and finally a model [41] of a Fluoride-salt-cooled high-temperature (FHR) reactor.

Lorenz system

The Lorenz system [42] is governed by:

$$\frac{dx}{dt} = \sigma(y - x), \quad \frac{dy}{dt} = x(\rho - z) - y, \quad \frac{dz}{dt} = xy - \beta z, \quad (9)$$

where x , y , and z are the state variables, whereas σ , ρ , and β are the system parameters. We use the classical parameters of $\rho = 28$, $\sigma = 10$, $\beta = 8/3$, which lead to chaotic behaviour. For this numerical example, we provide random initial conditions with uniform distributions $x_0 \sim \mathcal{U}(-5, 5)$, $y_0 \sim \mathcal{U}(-5, 5)$, $z_0 \sim \mathcal{U}(-5, 5)$, where \mathcal{U} is the discrete uniform distribution in the interval $[-5, 5]$, to generate 100 time series for training and validation with a split ratio of 80:20. Each time series contains 10,000 time steps with a time-step size of $\Delta t = 0.01$ solved using a Runge–Kutta numerical solver. The test data is generated by integrating the system with new initial states of $x_0 = y_0 = z_0 = 6$ with independent perturbations ϵ_x , ϵ_y and ϵ_z where $\epsilon_i \sim \mathcal{N}(0, 1)$ for each variable. Note that $\mathcal{N}(0, 1)$ denotes a normal distribution with 0 average and a standard deviation of 1. We adopt the same time-step size and number of time steps of 10,000 to generate one time series as test data. We employ the relative l_2 -norm error ε to assess the prediction accuracy, which is expressed as:

$$\varepsilon = \frac{\|\mathbf{x} - \hat{\mathbf{x}}\|_2}{\|\mathbf{x}\|_2} \times 100\%, \quad (10)$$

where $\hat{\mathbf{x}} = (\hat{x}, \hat{y}, \hat{z})$ and $\mathbf{x} = (x, y, z)$ are the model prediction and the ground truth from numerical solver, respectively. Following the assessment in Ref. [30], we focus on the short-time accuracy and compute the error on the first 512 time steps of the test sequence. The time window in which the error is computed is then $T_\varepsilon = 5.12$. We also assess the computation time of training (t_c) and number of floating-point operations (N_f) for one forward propagation with batch size of 1. We summarize the results in the supplementary material, where the proposed model using dense easy attention yields the lowest error, 1.99%, demonstrating the superior performance of the easy-attention method applied on temporal-dynamics predictions. The LSTM model has the highest number of learnable parameters, but the lowest training time and number of floating-point operations. However, it yields the highest l_2 -norm error of 37.68%, which indicates that the LSTM model is not able to reproduce the correct dynamical behaviour over a long time given the same set up as the transformer. The dense-easy-attention model reduces the time for training by 17% and the computational complexity by 25% with respect to the self-attention-based model while surpassing the number of learnable parameters of the self-attention-based model. This is due to the fact that the dense-easy-attention module comprises $\alpha \in \mathbb{R}^{h \times p \times p}$ and $\mathbf{W}_V \in \mathbb{R}^{p \times d_{\text{model}}}$ while the self-attention module comprises $\mathbf{W}_Q, \mathbf{W}_K, \mathbf{W}_V, \mathbf{W}_C \in \mathbb{R}^{p \times d_{\text{model}}}$ which has fewer parameters in the present study. However the computational cost for the easy-attention models is lower than that of the self attention since the softmax and the inner product inside the latter are eliminated. Note that the model employing sparse easy attention exhibits an error of 2.79% while only having 52% of the learnable parameters of the self-attention-based transformer, which implies that the sparsification induced by an offset of 0 benefits the robustness of the easy-attention method applied to temporal-dynamics prediction. The sparsity is defined as follows: the α matrix has a number of non-zero diagonals equal to $2 \cdot \text{offset} + 1$. We also implement the averaged relative Euclidean norm error $\psi(t)$ between the ground truth and the prediction, which is proposed in Ref. [43]:

$$\psi(t) = \left\langle \frac{\|\mathbf{x}(t) - \hat{\mathbf{x}}(t)\|_2}{\langle \|\mathbf{x}(t)\|_2 \rangle_t} \right\rangle_{\text{ens}}, \quad (11)$$

where $\langle \cdot \rangle_{\text{ens}}$ and $\langle \cdot \rangle_t$ indicate ensemble averaging over 100 sets of time series and over 10,000 time steps, respectively. Note that the set of time series used for evaluation are again generated by integrating the system with new initial states of $x_0 = y_0 = z_0 = 6$ with independent perturbations ϵ_x , ϵ_y and ϵ_z where $\epsilon_i \sim \mathcal{N}(0, 1)$ for each variable. Fig. 2 depicts the evolution $\psi(t)$ for the different models. One can observe that the easy-attention-based transformer deviates from the ground truth later than the LSTM and the self-attention-based transformer in terms of short-term prediction. We adopt a threshold of $\psi = 0.4$ as an adequate agreement with respect to the reference trajectory, it can be observed that the transformers using easy attention and sparse easy attention produce accurate instantaneous predictions for 7.04 and 5.97 time units, respectively. However, the self-attention-based transformer and the LSTM yields 4.90 and 1.10 accurate instantaneous predictions, respectively. The results indicate that the easy-attention-based transformer outperforms the self-attention-based transformer and the LSTM for short-term prediction.

Moreover, it can be observed that all the models produce similar levels of accuracy for long-term predictions. Due to the chaotic behavior of the Lorenz system and the fact that the errors accumulate over time, we do not only aim to keep $\psi(t)$ low for large t , but to preserve the general trajectory dynamics. To this end, we report the so-called Lorenz map (see Ref. [42]) in Fig. 3. The Lorenz map shows the evolution of two consecutive maximum values of z for

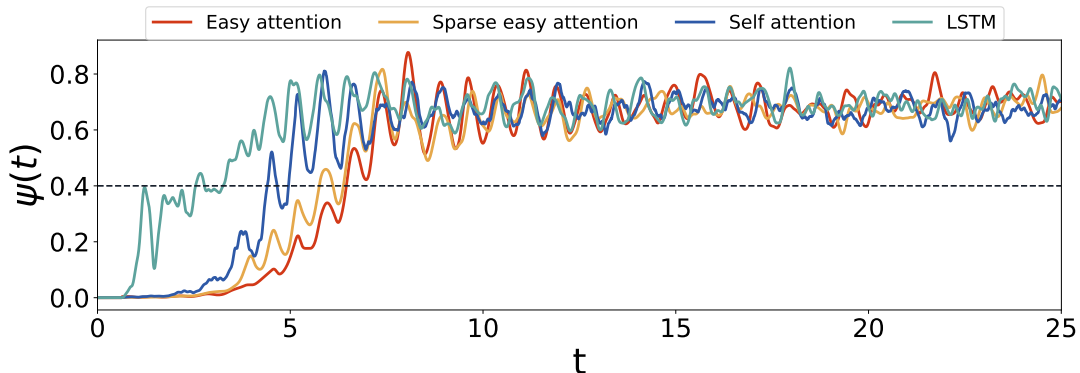


FIG. 2: **Assessment of short-term predictions for the various models.** Relative Euclidean norm of error $\psi(t)$ averaged over 100 sets of time series comprising 10,000 time steps, generated by integrating the system with new initial states of $x_0 = y_0 = z_0 = 6$ with independent perturbations ϵ_x , ϵ_y and ϵ_z where $\epsilon_i \sim \mathcal{N}(0, 1)$ for each variable. The dashed horizontal line shows the threshold value considered for accurate predictions, namely $\epsilon = 0.4$.

the various prediction methods. This figure shows that, while the two easy-attention-based transformers accurately reproduce the trend of the ground truth, the self-attention-based transformer shows some deviations and the trend from the LSTM significantly deviates with respect to the reference.

Furthermore, we compute the dominant Lyapunov exponent using the method described in Ref. [21] to further examine to what extent the various methods can reproduce the sensitivity in the chaotic behavior of the reference chaotic system. For two time series, 1 and 2, we define the deviation of their respective trajectories in terms of the Euclidean norm:

$$|\delta\mathbf{A}(t)| = \left[\sum_{i=1}^3 (x_{i,1}(t) - x_{i,2}(t))^2 \right]^{\frac{1}{2}}, \quad (12)$$

and we denote the separation at $t = t_0$ as $|\delta\mathbf{A}_0|$. The initial divergence of both trajectories can be assumed to behave as $|\delta\mathbf{A}(t')| = \exp(\lambda t')|\delta\mathbf{A}_0|$, where λ is the so-called Lyapunov exponent and $t' = t - t_0$. In the present study we introduced a perturbation, with norm $|\delta\mathbf{A}_0| = 10^{-6}$ at $t_0 = 400$, where all the variables are perturbed, and subsequently we analyzed its divergence with respect to the unperturbed trajectory. Fig. 3 (bottom) depicts the Lyapunov exponents obtained for the Lorenz system and models via ensemble averaging 10 perturbed test datasets with initial states of $x_0 = y_0 = z_0 = 6$, and predictions done after $t = 500$ with the studied models.

The easy-attention based transformer yields a comparable Lyapunov exponent of $\lambda = 0.919$, which is in very good agreement with the ground truth of $\lambda = 0.929$ and other numerical approximations [44]. This indicates that the model learns the chaotic nature of the Lorenz system. However, the model using sparse easy attention yields $\lambda = 0.823$, deviating from the ground truth. One possible reason is the reduction of parameters in the attention module, which leads to the model becoming not sensitive enough to detect the separation of the trajectories via perturbation. It can be stated, the easy-attention performance relies solely on the quality of the available data. Given richer training data it could be possible to improve the prediction of the Lyapunov exponent, replicating more realistic behaviors.

Furthermore, Fig. 4 depicts the probability density functions (PDF) of the x and z variables. To highlight the entire path and avoid focusing near $(0, 0, 0)$, an arc-length parametrization is performed to $\mathbf{x}(t) = (x(t), y(t), z(t))$ to obtain a natural curve $\hat{\mathbf{x}}(s) = \mathbf{x}[t(s)]$. This is done by considering $t(s)$, the inverse function of $s(t) = \int_0^t \|\mathbf{x}'(r)\|_2 dr$. As before, the models with the most similar PDF to the one of the test data are the two easy-attention-based transformers. Both exhibit a better performance when considering the symmetry on the x axis, as shown below. It is necessary to mention the importance of replicating symmetries when learning chaotic systems as the main exoticism of complex systems relies on their unique structures, spatially; attractors and spatio-temporally, probability density functions. Being able to reproduce such structures it is not a trivial consequence of the training procedure: while the model has as single objective temporal predictions, inspecting the results in Fig. 4 one can conclude that not only the space is well reconstructed but the velocity, the time derivative of the state variable too, as the frequency per volume unit is also learned. In Fig. 4 we depict the embedded manifold given by the joint PDF (JPDF). Note the excellent agreement with the ground truth observed after the symmetry transformation. The possibility of accurately reproducing spatio-temporal structures will become critical in more challenging chaotic problems such as turbulence. Compared with the self-attention-based transformer, the transformers using easy attention have the lowest computa-

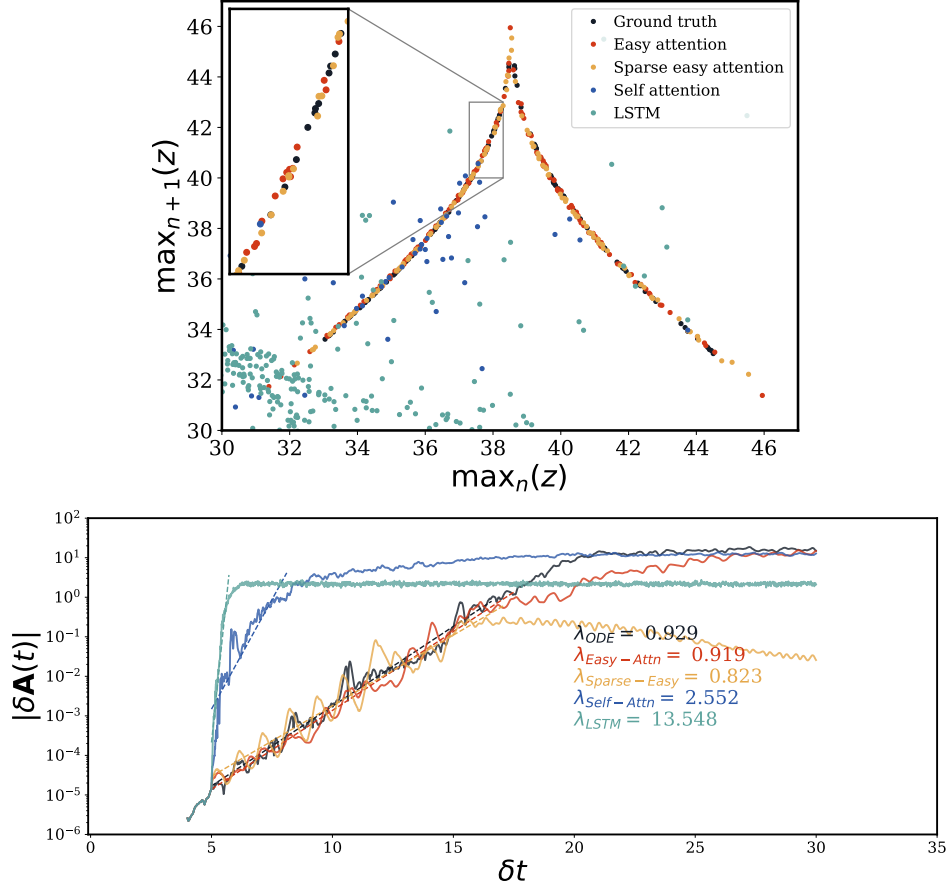


FIG. 3: **Characterization of the dynamics of the Lorenz system.**(Top) The Lorenz map representing the two consecutive local maxima of z produced by each model. Note that we amplify the region where $\max_n(z) \in (37.3, 38.3)$ and $\max_{n+1}(z) \in (40, 43)$. (Bottom) Leading Lyapunov exponents obtained by adding a perturbation at time step of 400 with a magnitude of $\delta = 1 \times 10^{-6}$. Note that we report the obtained Lyapunov exponents by ensemble averaging 10 perturbed test dataset with initial states of $x_0 = y_0 = z_0 = 6$ whereas ODE denotes the results obtained by Lorenz system. The obtained Lyapunov exponents were scaled by the adopted time step $\Delta t = 0.01$ in the present study, and Δt denotes the time after the introduction of the perturbation. The dashed lines denote the fitted exponential evolution used to obtain the corresponding Lyapunov exponents.

tional cost for training and exhibit higher accuracy on reproduction of long-term dynamics, which indicates that the transformer models using easy attention are more robust for temporal-dynamics prediction than the model using self attention.

Low-order model of turbulence shear flows

We now use the easy-attention-based seq2one transformer model to predict a more complex chaotic system with a higher dimension of 9, namely the low-order representation of near-wall turbulence described by the model proposed by Moehlis *et al.* [40]. The system comprises nine spatial modes $\mathbf{u}_n(\mathbf{x})$ which represent the velocity mean profile, streamwise vortices, the streaks and their instabilities as well as their coupling [43].

In this model, the Reynolds number Re is defined in terms of the laminar velocity U_0 at a distance of $h/2$ from the top wall where the full height of channel is h . In the present study, following the previous studies [21, 43], we consider $Re = 400$ and employ U_0 and h as velocity and length scales, respectively. The ODE model was used to produce over 10,000 time series of the nine amplitudes, each with a time span of 4,000 time units, for training and validation with a ratio of 80:20. The domain size is $L_x = 4\pi$, $L_y = 2$ and $L_z = 2\pi$, where x , y and z are the streamwise, wall-normal and spanwise coordinates respectively, and we consider only time series that are chaotic over the whole time span, which means that we do not consider relaminarized cases. The instantaneous velocity field is given by

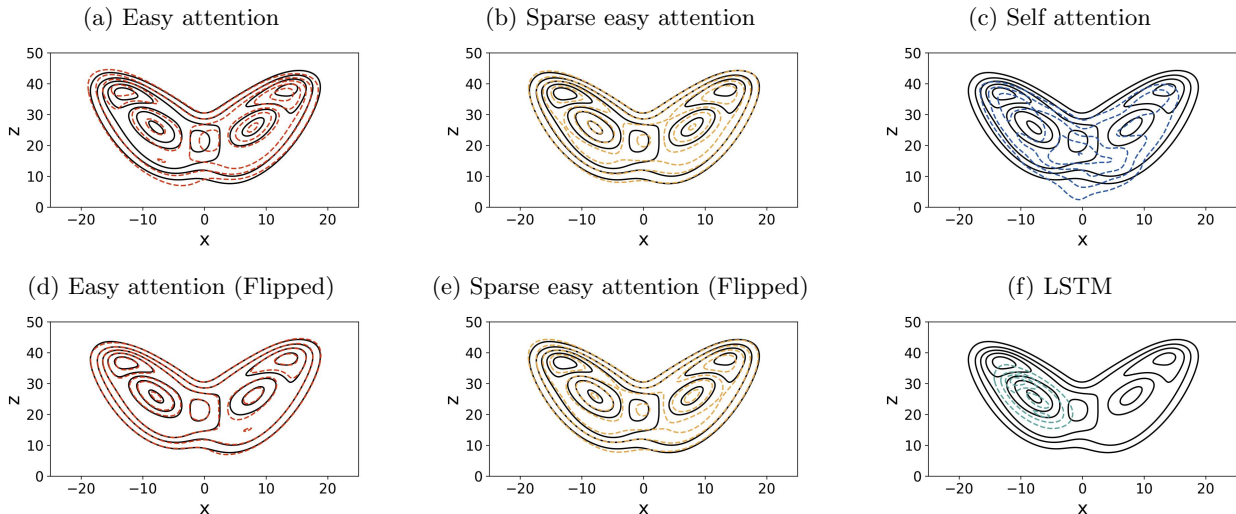


FIG. 4: Joint contour plots of the probability density functions of variables x and z of the Lorenz system and predictions using different models. Note that the trajectory has been parametrized by the arc length and the prediction is flipped on the x axis in the bottom panels showing easy-attention models.

$\mathbf{u}(\mathbf{x}, t) = \sum_{m=1}^9 a_m(t) \mathbf{u}_m(\mathbf{x})$, where $\mathbf{x} = (x, y, z) \in D \subseteq \mathbb{R}^3$ denotes the spatial coordinates, $t \in [0, T_{\max}]$ the time and D is the spatial domain. From the incompressible Navier–Stokes equations, the free-slip boundary conditions, and computing the Galerkin projections, the following system of ordinary differential equations for the amplitudes $a_m(t)$ is obtained:

$$\begin{aligned} \frac{da_1}{dt} &= -\eta_1 + \eta_1 a_1 + \phi_1(a_1, a_2, \dots, a_9), \\ \frac{da_m}{dt} &= \eta_m a_m + \phi_m(a_1, a_2, \dots, a_9) \quad m = 2, 3, \dots, 9. \end{aligned} \quad (13)$$

As introduced above, we will investigate the transformer’s ability to reconstruct and capture both temporal and spatial dynamics for this turbulent shear flow. We will use essentially the same architecture as that used for the Lorenz system, changing the embedding module from time2vec to the time-space embedding module proposed in Refs. [31, 45], see the Supplementary Material for additional details. We will also compare these results with the one-layer LSTM architecture reported in Ref. [43].

In Fig. 5 (top) we show the PDF of the Poincaré section with $a_2 = 0$ (and $da_2/dt < 0$) for variables a_1 and a_3 . It can be observed that both the easy-attention-based transformers and the LSTM reconstruct accurately the spatial behavior depicted by the reference Poincaré section. On the other hand, the self attention does not exhibit the level of accuracy produced by the other models. Furthermore, Fig. 5 (bottom) shows reference and predicted turbulence statistical quantities, *i.e.* the streamwise mean velocity profile \bar{u} , the streamwise velocity fluctuations $\overline{u'^2}$ and the Reynolds shear stress $\overline{u'v'}$. These quantities are obtained by averaging 500 time series spanning 4,000 time units each with $\Delta t = 0.01$ and over the periodic directions x and z . Our results show that the LSTM yields the best reconstruction for the mean velocity with a relative error of 0.45% while the easy attention remains the most accurate when studying the streamwise velocity fluctuations: 0.42%. Taking this into account and considering the superior robustness of the easy attention exemplified in the Lorenz system, it can be concluded that easy-attention-based transformer outperforms the self attention when predicting this turbulent-flow model. The sparse easy attention shows really promising results when considering how the accuracy of the results is not affected drastically by the parameter reduction induced by the sparsity imposed on the attention matrix. Based on the results reported here, easy attention remains the preferable model as it slightly underperforms LSTM networks when reconstructing the streamwise mean velocity by 0.37 percentage points (pp) but outperforms the latter by 2.07 pp considering the streamwise velocity fluctuations. When studying complex systems through deep learning it is important to carefully select the loss function. In the present work all the models are trained with the purpose of obtaining, an accurate reconstruction and prediction of the next step in the temporal series, a goal which is represented by Eq. (3). Improved performance in other metrics may be possible by properly designing the training stage [46], leveraging topological studies on the different realizations explored during the training stage.

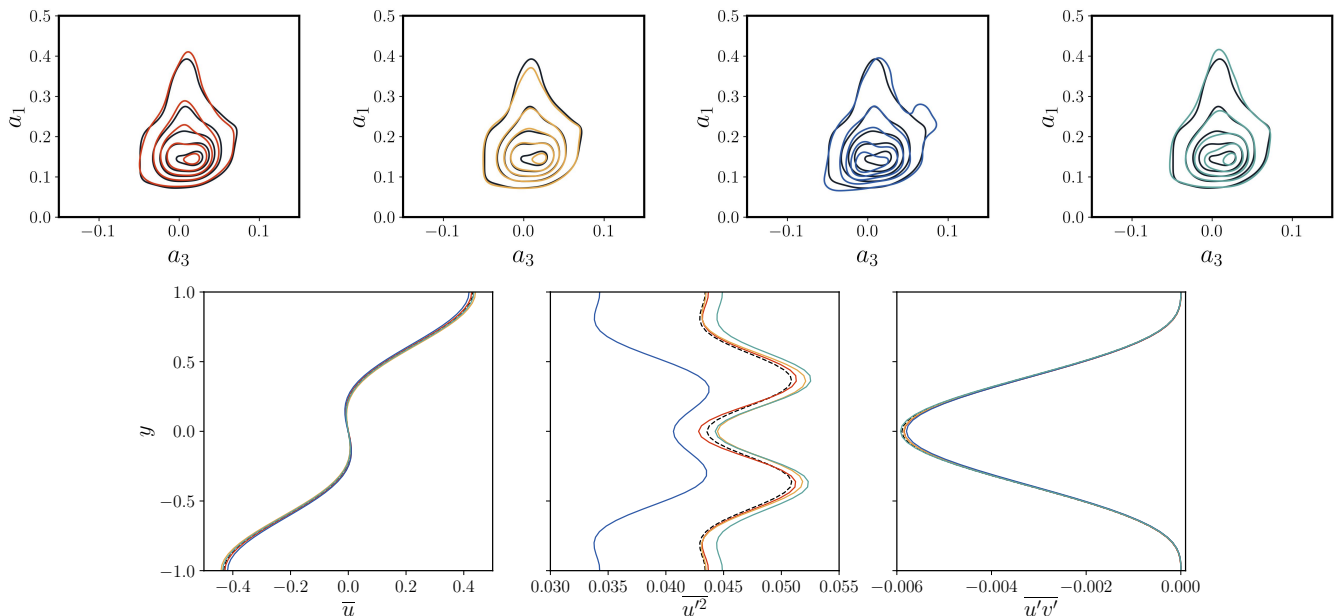


FIG. 5: **Turbulent-flow predictions by the various methods.** (Top) Probability density function of the Poincaré maps showing the intersection with $a_2 = 0$ plane (with $da_2/dt < 0$). In all the cases black denotes the ground truth while the colors correspond to predictions based on (from left to right): easy attention, sparse easy attention, self attention and LSTM. (Bottom) Turbulence statistics corresponding to (left) streamwise mean profile, (middle) streamwise velocity fluctuations and (right) Reynolds shear stress. Colors correspond to the cases on the top panels.

Model of a Nuclear Reactor

To conclude the assessment of our easy-attention-based model, we will consider a more complex problem of industrial relevance: a model of a nuclear reactor. In particular, we will evaluate the feasibility of using easy attention as a surrogate model to predict the temporal evolution of the state variables in the reactor in order to increase safety and decrease operational costs. The pebble-bed fluoride-salt-cooled high-temperature (PB-FHR) reactor under study here is a Generation-IV nuclear reactor [47] that utilizes a liquid salt coolant, solid fuel pebbles and a graphite moderator. The fluoride-salt coolant has attractive properties that motivate the FHR design both economically and safety-wise, including high boiling point, low operational pressure and high heat-transfer efficiency [48]. We will consider the generic FHR (gFHR), a publicly accessible benchmark model created by Kairos Power [41] which retains the main neutronics and thermal-hydraulics information of their proprietary Kairos Power FHR (KP-FHR) model. Data is generated with the System Analysis Module (SAM), a tool developed by Argonne National Laboratory for whole-plant transient analysis of advanced reactor concepts [49]. The SAM gFHR model considered here was developed using a hybrid method [50] that combines high-fidelity neutronics simulations and intermediate-fidelity thermal-hydraulics simulations for an entire-plant representation of the reactor configuration. In this study we will focus on predicting the temporal evolution of 13 state variables, and more details regarding the employed datasets can be found in the Supplementary Material.

All variables are computed by the benchmark model introduced above, considering the latter as the reference.

In the Supplementary Material we show the temporal evolution for several reactor variables, together with predictions from the various models. In Fig. 6 (top) we depict the PDF of the Core Flow of the reactor, which is one of the most relevant operation variables in determining reactor performance. The easy-attention model exhibits the best reconstructive capability when comparing with the ground-truth data, while the sparse easy attention significantly over predicts the peaks towards the left and under predicts the ones on the right. On the other hand, the self-attention model can reproduce the peaks reasonably well, but the tails of the distribution surpass the limits of the steady-state distribution. In Fig. 6 (bottom), we show the power-spectral density for both the Core Flow and the Core Energy. Once again, the easy-attention model exhibits the best predictions considering both the position and magnitude of the predicted spectral peak. The self-attention model yields reasonably accurate results for low frequencies, but it introduces a second peak. Both the LSTM and sparse-easy-attention models lack the level of accuracy exhibited by the other two models, with the sparse-easy-attention yielding a slightly better qualitative agreement with the

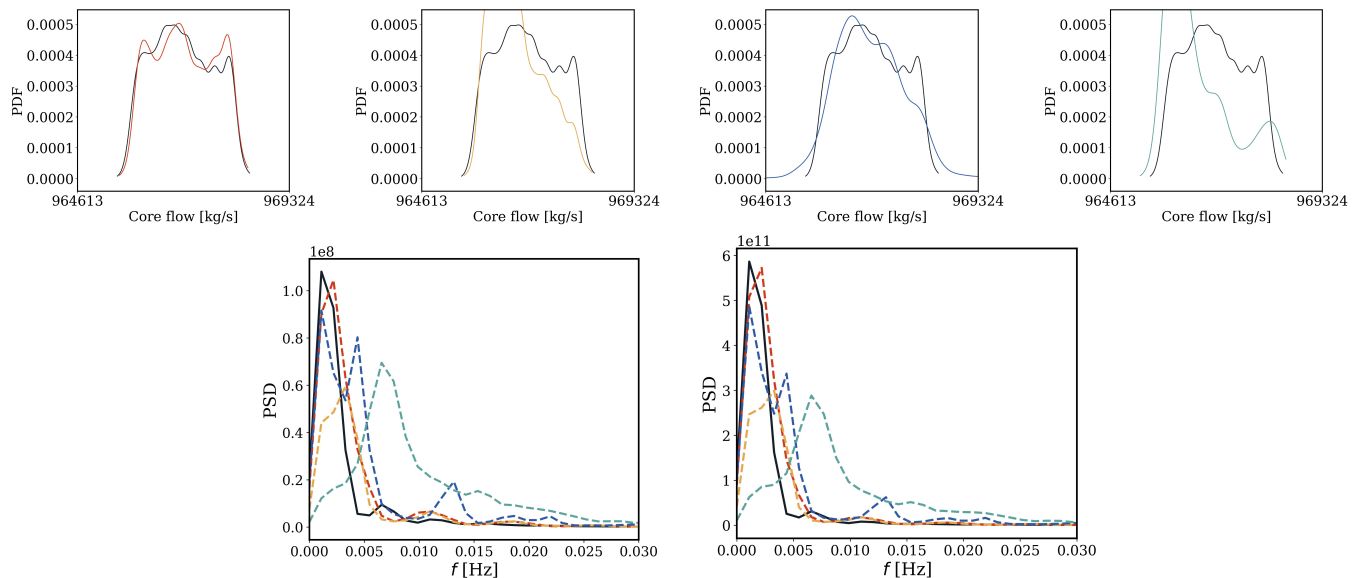


FIG. 6: **Characterization of variables in a nuclear reactor reconstructed by the various prediction methods.** (Top) Probability density function of the Core Flow. In all the cases black denotes the ground truth while the colors correspond to predictions based on (from left to right): easy attention, sparse easy attention, self attention and LSTM. (Bottom) Power-spectral density of (left) Core Flow and (right) Core Energy, where f represents frequency. Colors as in the top panels.

reference than the LSTM. This behavior highlights the importance of the α matrix in the transformer encoder, as it is responsible for learning temporal dependencies between time instances.

Summary and conclusions

We proposed a novel attention mechanism for transformer neural networks, namely the easy attention, which does not rely on queries and keys to generate attention scores and eliminates the nonlinear softmax function. The easy attention arises from the nonelastic nature of the trace, as this makes impossible any backwards traceability of the information, decreasing the relevance of the exact value of each matrix element. Taking this into account, we propose to learn the attention scores α directly, instead of learning the query and key matrices, removing the \mathbf{W}_K , \mathbf{W}_Q and softmax from the attention mechanism, yielding a considerable reduction in the numbers of parameters. Furthermore, we propose the sparse-easy-attention method, which reduces the number of learnable parameters of the tensor α by only learning the (near-) diagonal elements. We also propose a method to perform multi-head easy attention which employs multiple α to improve the long-term predictions. Considering chaotic systems as our predictive problem, the invariant nature of attractors and the sensitivity to small perturbations on the initial conditions, suggest that it may be more convenient to use an input-independent model. In future works we will expand the interpretability of the model with operator theory [51], leveraging ideas from both Koopman Operator Theory and quantum mechanics, specifically the Schrödinger equation, where the operator evolving the observable is input independent.

We first study sinusoidal functions and we investigate the core idea of self-attention by implementing SVD on the $\mathbf{Q}^T \mathbf{K}$ product and the softmax attention score. The results reveal that the self attention in fact compresses the input sequence transformed covariance matrix. Following this observation, we propose our easy-attention mechanism. For input transform-wave reconstruction, the easy-attention model achieves 0.0018% l_2 -norm error with less computation time for training and complexity than self attention, which exhibits an l_2 -norm error of 10%. Motivated by the promising performance on sinusoidal-wave reconstruction, we propose the multi-easy-attention method, which combines the discrete Fourier transform with attention mechanism for signal reconstruction. The unique capability of easy attention to learn long-term dynamics for periodic signals suggests that this method may have great potential for additional applications, such as signal de-noising.

Subsequently, we apply easy attention in the proposed transformer model for temporal-dynamics prediction of chaotic systems and we investigate the performance of our models on the Lorenz system. The transformer model with dense easy attention yields the lowest relative l_2 -norm error of 2.0%, outperforming the same transformer architecture with the self attention (7.4%) and the LSTM model (37.7%). Furthermore, when inspecting the nine-equation model of

wall-bounded turbulence by Moehlis *et al.* [40] the long-term statistics discussed in the Supplementary Material show how LSTM yields very similar performance in the mean flow compared with the easy attention. Regarding the PDF of the Poincaré section shown in Fig. 5, the easy attention also exhibits better predictions than the other models, in particular when accounting for the existing symmetries observed in Fig. 4 (top). Therefore, the easy attention arises as the most accurate model when studying chaotic systems. Regarding the studied model of a nuclear reactor, the easy attention shows the best reconstructive capability when considering PSD and PDF analysis. The results also show that, compared with the self-attention-based transformer, the transformers using easy attention have a much lower computational cost, exhibit less complexity and have less parameters. Thus the transformer model using easy attention is more robust for temporal-dynamics predictions.

Furthermore, a significant advantage of the easy-attention-based transformer is its accurate reconstruction of the invariant sets, as shown in Figs. 4,6. These invariant sets arise when inspecting the systems independently of time, as the latter converge to a stationary probability density function and a fixed attractor in state space. As the PDF is reconstructed, although our temporal prediction diverges, the density of information per neighborhood is accurately represented by the easy-attention model. Taking into account the shadowing lemma [52], it can be stated that the prediction given by the transformer can be trusted to represent the orbits of the dynamical system, since the diverged orbit remains as a pseudo-orbit infinitely close to another orbit on the original system.

In conclusion, the easy-attention mechanism, due to its robustness, exhibits promising performance in the tasks of signal/trajectory reconstruction as well as temporal-dynamics prediction in chaotic systems. Our results also indicate potential for application in more complex large-scale dynamical systems, since transformer networks are naturally designed for high-dimensional sequence data [25, 30–33].

Methods

In this section, we will focus on the mathematical development of the attention part of the model and its implications on the final output, since the other blocks follow the standard transformer architecture [26]. To this end we will first examine the self-attention model and later explain in detail the easy-attention method. The mathematical implementation of a transformer encoder block is expressed as follows [53]: a transformer block is a parameterised function $T : \mathbb{R}^{n \times d} \rightarrow \mathbb{R}^{n \times d}$, usually consisting of an attention part and a feed forward-network, both with residual connections and normalization layer, see the transformer block used for each case in the Supplementary Material.

Notation

Adhering to the customary notation, given any matrix $\mathbf{A} \in \mathbb{R}^{n \times d}$, $[\mathbf{A}]_{ij}$ will denote the element on the i -th row and j -th column of \mathbf{A} and given a vector $\mathbf{a} \in \mathbb{R}^d$, $[\mathbf{a}]_j$ will denote its j -th component. We represent by lowercase \mathbf{a}_i the i -th row of any matrix \mathbf{A} . As it is usual, we will interpret all vectors, such as $\mathbf{a}_i \in \mathbb{R}^d$, as column vectors. Thus, assuming a concatenation by columns and wrote formally, $\mathbf{A} = (\text{concat}\{\mathbf{a}_i\}_{i=1}^n)^T$. In the following we will assume that $\mathbf{X} \in \mathbb{R}^{n \times d}$ is the input of the model, composed by the past n observations of d features each. For example, in the Lorenz case $n = d = 64$ (after the time embedding).

Attention

Let us focus on the attention sub-block, which is in turn another transformation $\mathbb{R}^{n \times d} \rightarrow \mathbb{R}^{n \times d}$, $\mathbf{X} \mapsto \hat{\mathbf{X}}$. That mapping, applied to each row of \mathbf{X} , takes the following form:

$$\hat{\mathbf{x}}_i = \sum_{j=1}^n \alpha_{i,j} \mathbf{W}_V^T \mathbf{x}_j. \quad (14)$$

The matrix \mathbf{W}_V applies the same linear transformation into the input \mathbf{x}_i . Denoting as $\boldsymbol{\alpha} \in \mathbb{R}^{n \times n}$ the matrix formed by the α_{ij} values, *i.e.* $[\boldsymbol{\alpha}]_{ij} = \alpha_{ij}$ and $\mathbf{W}_V \in \mathbb{R}^{d \times k}$ where $k = d$ for our study:

$$\begin{aligned} [\hat{\mathbf{X}}]_{ik} &= [\hat{\mathbf{x}}_i]_k = \sum_{j=1}^n \alpha_{ij} [\mathbf{W}_V^T \mathbf{x}_j]_k = \sum_{j=1}^n \sum_{l=1}^n \alpha_{ij} [\mathbf{W}_V^T]_{kl} [\mathbf{x}_j]_l \\ &= \sum_{l=1}^n [\mathbf{W}_V^T]_{kl} [\boldsymbol{\alpha} \cdot \mathbf{X}]_{il} = \sum_{l=1}^n [\boldsymbol{\alpha} \cdot \mathbf{X}]_{il} [\mathbf{W}_V]_{lk} = [\boldsymbol{\alpha} \cdot \mathbf{X} \cdot \mathbf{W}_V]_{ik}. \end{aligned}$$

Therefore the model can be written in a matrix form as:

$$\hat{\mathbf{X}} = \boldsymbol{\alpha} \mathbf{X} \mathbf{W}_V. \quad (15)$$

In Eq. (15) it can be clearly seen that \mathbf{W}_V and $\boldsymbol{\alpha}$ are a spatial and a temporal transformation, respectively.

Self-attention

In the standard implementation of the transformer [26] the attention is computed using a scaled dot-product attention as follows. Given an input \mathbf{X} , the query, key and value of each observation are computed respectively as

$$\mathbf{Q}(\mathbf{x}_i) = \mathbf{W}_Q^T \mathbf{x}_i, \quad \mathbf{K}(\mathbf{x}_i) = \mathbf{W}_K^T \mathbf{x}_i, \quad \mathbf{V}(\mathbf{x}_i) = \mathbf{W}_V^T \mathbf{x}_i. \quad (16)$$

These quantities are constructed based on three different weight matrices: $\mathbf{W}_Q, \mathbf{W}_K, \mathbf{W}_V \in \mathbb{R}^{k \times d}$. These matrices project each observation into a vector in a latent space of dimension k (at the moment assume $k = d$) and are all learned during training. The attention score $\alpha_{i,j}$, that correlates the observation \mathbf{x}_i with \mathbf{x}_j , is computed as:

$$\alpha_{i,j} = \text{softmax} \left(\frac{\langle \mathbf{Q}(\mathbf{x}_i), \mathbf{K}(\mathbf{x}_j) \rangle}{\sqrt{k}} \right); \quad \text{softmax}(\mathbf{z}_j) = \frac{\exp(\mathbf{z}_j)}{\sum_{k=1}^n \exp(\mathbf{z}_k)}, \quad (17)$$

in which softmax is applied to each row of $\boldsymbol{\alpha}$. That well-known activation function is a generalization of the logistic function used for compressing d -dimensional vectors of arbitrary real entries into real vectors of the same dimension in the range $[0, 1]$, with normalized l_1 -norm. Once the attention scores are computed, using Eq. (14) the output of the module is obtained.

It is possible represent the product $\mathbf{W}_V^T \mathbf{x}_i$ (assuming \mathbf{W}_V to be square, as discussed below) as a linear combination of the eigenvectors and eigenvalues $(\mathbf{v}_k, \lambda_k)$ of \mathbf{W}_V for unique coefficients $c_{k,j}$ depending only on \mathbf{x}_j , resulting on:

$$\hat{\mathbf{x}}_i = \sum_{j=1}^n \alpha_{i,j} \mathbf{V}(\mathbf{x}_j) = \sum_{j=1}^n \alpha_{i,j} \left(\sum_{k=1}^n \lambda_k \mathbf{v}_k c_{k,j} \right). \quad (18)$$

For analytical purposes in Fig. 1(c) we will express the inner product inside the softmax operation in terms of the trace so it is possible to take advantage of its cyclic property:

$$\alpha_{i,j} = \text{softmax} \left(\frac{\text{Tr}(\mathbf{W}_Q \mathbf{W}_K^T \mathbf{x}_j \mathbf{x}_i^T)}{\sqrt{k}} \right). \quad (19)$$

In this study we asses the importance of the weight matrices for the accuracy of the predictions and note that the result depends on the eigenvalues of $\mathbf{W}_Q \mathbf{W}_K^T \mathbf{x}_j \mathbf{x}_i^T$. Given the nature of the trace, introduced in the interpretation of the attention mechanism, the transformer only uses the final result of the sum. For example: let $\mathbf{Z} \in \mathbb{R}^{n \times n} \Rightarrow \text{Tr}(\mathbf{Z}) = a + b + c = d$, where $a, b, c, d \in \mathbb{R}$, and in principle there are infinite possible values of a, b, c such that the sum is equal to d .

Note that in the general attention mechanism the query, key and value can be computed using different input observations, $\mathbf{Q}(\mathbf{x}_i)$, $\mathbf{K}(\mathbf{y}_i)$, and $\mathbf{V}(\mathbf{z}_i)$. This is the case of, for example, translation models in which the original words are compared with the translated ones, leading to an attention matrix that correlates the original and translated words (observations), see Ref. [26]. In our temporal prediction case, the only relevant information is the past observations, so the values in Eq. (16) are all computed for the same observations \mathbf{x}_i .

Easy attention

In the easy-attention mechanism, the key and query of self attention are eliminated, and (14) is computed directly. We directly learn $\boldsymbol{\alpha} \in \mathbb{R}^{n \times n}$ as a learnable attention-score tensor of the spanned eigenspace of the multiplication of the time-delay input matrix by its transpose. As consequence, only $\boldsymbol{\alpha}$ and \mathbf{W}_V are required to be learned. In particular, an input \mathbf{x} is projected as the value tensor \mathbf{V} by \mathbf{W}_V . Subsequently, we compute the product of \mathbf{V} and the attention scores $\alpha_{i,j}$ as the output $\hat{\mathbf{x}}_i$. The matrix formula version in Eq. (15), together with the fact that the attention scores are constant, suggest that $\hat{\mathbf{X}}$ is a rewriting of \mathbf{X} choosing another basis (ideally, the best) for time ($\boldsymbol{\alpha}$) and features (\mathbf{W}_V).

As the attention scores are fixed once trained, they remain constant during the prediction process, as if the values $\langle \mathbf{Q}(\mathbf{x}_i), \mathbf{K}(\mathbf{x}_j) \rangle$ only depend on i and j but not on the inputs \mathbf{x}_i and \mathbf{x}_j . This non-trivial assumption, which may not be

applicable to scenarios where the inputs could be presented in different orders, is powerful in time-series prediction, since the information is always provided in the same way: the (ordered) past observations. However, considering time series sampled with a non-uniform time step, seems reasonable not to consider the inner product as measure for quantifying correlation, since the distance in the real vector space between vector elements does not consider the different sampling rate of the given elements in the state space neither the rate of information propagation. Moreover, as the order of the inputs \mathbf{x}_i is always the same, an encoding of the position of each \mathbf{x}_i is not needed, enabling the use of embedding instead.

Furthermore, α can be sparsified by only learning the diagonal elements, or adding elements in off-diagonal positions both above and below the main diagonal if necessary, which further reduces the number of learnable parameters of the easy-attention mechanism. At the stage of forward propagation or inference, those parameters are assigned to the corresponding indices in a matrix of dimension $\mathbb{R}^{n \times n}$. At the Supplementary material one can find illustrations to further differentiate between the dense and sparse easy-attention methods. In the present study, we only consider learning main-diagonal elements as sparsification.

Multi-head strategies

To conclude the study, we will introduce the implementation of the easy attention with multi-head strategies. Assume now that the attention mechanism is computed h times and the concatenated, as follows: Then,

$$\hat{\mathbf{X}} = \text{concat} \left\{ \alpha^l \mathbf{X} \mathbf{W}_V^l \right\}_{l=1}^h. \quad (20)$$

Note that it is common to consider a smaller dimension on the value space: $\mathbf{W}_V^l \in \mathbb{R}^{k \times d}$, while α^l remains to be in $\mathbb{R}^{n \times n}$. The matrix with all the values, $\mathbf{V}^l(\mathbf{X}) = \mathbf{X} \cdot \mathbf{W}_V^l$, which needs to be determined for each head, can be computed for all of them together as $\mathbf{V}(\mathbf{X}) = \text{concat}\{\mathbf{V}^l(\mathbf{X})\}_{l=1}^h = \mathbf{X} \mathbf{W}_V$, where $\mathbf{W}_V = \text{concat}\{\mathbf{W}_V^l\}_{l=1}^h$, and then, $\hat{\mathbf{X}} = \text{concat}\{\alpha^l \cdot \mathbf{V}^l(\mathbf{X})\}_{l=1}^h$. See the Supplementary Material for additional details. This allows to consider only one \mathbf{W}_V square matrix as in the single-head case.

In the most general case of multi-head self-attention, another matrix $\mathbf{W}_O \in \mathbb{R}^{k \cdot h \times d}$ is added to (20), as $\hat{\mathbf{X}} = \text{concat}\{\alpha^l \mathbf{X} \mathbf{W}_V^l\}_{l=1}^h \mathbf{W}_O$. This process is also omitted in the easy attention case.

Compared with the previous one-head formula, it can be observed that any modification on the features (right-matrix multiplication by \mathbf{W}_V^T) remains the same, but the time transformation (left-matrix multiplication by α) now depends also on the (group of) feature variables. The multi-head easy attention is beneficial to preserve long-term dependencies when d becomes large. The mechanisms of single- and multi-head easy attention are illustrated in the Supplementary Material.

Computation

In the present study, all the model training and testing are implemented on a single central-processing unit (CPU) from a machine with the following characteristics: AMD Ryzen 9 7950X with 16 cores, 32 threads, 4.5 Ghz and 62 GB RAM. All machine-learning models and experiments were conducted using the PyTorch framework [54] (version 2.0.0). PyTorch was chosen due to its flexibility, ease of use, and extensive support for deep learning research. The custom models and neural-network architectures used in this work were implemented using PyTorch’s modular design, allowing seamless composition of layers and custom components. All the data and codes will be made available open access upon publication of the manuscript in the following repository: <https://github.com/KTH-FlowAI>

Acknowledgments

R.V. acknowledges financial support from ERC grant no. ‘2021-CoG-101043998, DEEPCONTROL’ and the EU Doctoral Network MODELAIR. Part of the ML-model testing was carried out using computational resources provided by the National Academic Infrastructure for Supercomputing in Sweden (NAISS). Jasmin Lim and Karthik Duraisamy are supported by APRA-E under the project *SAFARI: Secure Automation for Advanced Reactor Innovation* at the University of Michigan. Roger Arnau was supported by a contract of PAID-01-21 from the Universitat Politècnica de València. The authors would like to thank to Prof. Igor Mezić for helpful feedback on the manuscript.

References

-
- [1] F. Takens, Detecting strange attractors in turbulence, in *Dynamical Systems and Turbulence, Warwick 1980*, edited by D. Rand and L.-S. Young (Springer Berlin Heidelberg, Berlin, Heidelberg, 1981) pp. 366–381.
- [2] I. Mezić and A. Banaszuk, Comparison of systems with complex behavior, *Physica D: Nonlinear Phenomena* **197**, 101 (2004).
- [3] H. Arbabi and I. Mezić, Ergodic theory, dynamic mode decomposition, and computation of spectral properties of the koopman operator, *SIAM Journal on Applied Dynamical Systems* **16**, 2096 (2017).
- [4] S. Pan and K. Duraisamy, On the structure of time-delay embedding in linear models of non-linear dynamical systems, *Chaos: An Interdisciplinary Journal of Nonlinear Science* **30**, 073135 (2020).
- [5] J. Lumley, The structure of inhomogeneous turbulent flows, In: Yaglom, A.M. and Tartarsky, V.I., Eds., *Atmospheric turbulence and radio wave propagation* **23**, 166 (1967).
- [6] A. Towne, O. T. Schmidt, and T. Colonius, Spectral proper orthogonal decomposition and its relationship to dynamic mode decomposition and resolvent analysis, *Journal of Fluid Mechanics* **847**, 821–867 (2018).
- [7] P. J. Schmid, Dynamic mode decomposition of numerical and experimental data, *Journal of Fluid Mechanics* **656**, 5–28 (2010).
- [8] S. Le Clainche and J. M. Vega, Higher order dynamic mode decomposition, *SIAM Journal on Applied Dynamical Systems* **16**, 882 (2017).
- [9] I. Mezić, Spectral properties of dynamical systems, model reduction and decompositions, *Nonlinear Dynamics* **41**, 309 (2005).
- [10] B. O. Koopman and J. v. Neumann, Dynamical systems of continuous spectra, *Proceedings of the National Academy of Sciences* **18**, 255 (1932).
- [11] S. Pan and K. Duraisamy, Physics-informed probabilistic learning of linear embeddings of nonlinear dynamics with guaranteed stability, *SIAM Journal on Applied Dynamical Systems* **19**, 480–509 (2020).
- [12] C. W. Rowley, I. Mezić, S. Bagheri, P. Schlatter, and D. S. Henningson, Spectral analysis of nonlinear flows, *Journal of Fluid Mechanics* **641**, 115–127 (2009).
- [13] B. Lusch, J. N. Kutz, and S. L. Brunton, Deep learning for universal linear embeddings of nonlinear dynamics, *Nature communications* **9**, 4950 (2018).
- [14] M. A. Khodkar, P. Hassanzadeh, and A. Antoulas, A Koopman-based framework for forecasting the spatiotemporal evolution of chaotic dynamics with nonlinearities modeled as exogenous forcings (2019), [arXiv:1909.00076](https://arxiv.org/abs/1909.00076).
- [15] P. Bevanda, S. Sosnowski, and S. Hirche, Koopman operator dynamical models: Learning, analysis and control, *Annual Reviews in Control* **52**, 197 (2021).
- [16] H. Eivazi, L. Guastoni, P. Schlatter, H. Azizpour, and R. Vinuesa, Recurrent neural networks and Koopman-based frameworks for temporal predictions in a low-order model of turbulence, *International Journal of Heat and Fluid Flow* **90**, 108816 (2021).
- [17] G. Box and G. M. Jenkins, *Time series analysis forecasting and control*, 4th ed. (Wiley, 2008).
- [18] I. Goodfellow, Y. Bengio, and A. Courville, *Deep learning* (MIT Press, 2016).
- [19] S. Hochreiter and J. Schmidhuber, Long short-term memory, *Neural Computation* **9**, 1735 (1997).
- [20] K. Hasegawa, K. Fukami, T. Murata, and K. Fukagata, Machine-learning-based reduced-order modeling for unsteady flows around bluff bodies of various shapes, *Theoretical and Computational Fluid Dynamics* **34**, 367 (2020).
- [21] P. A. Srinivasan, L. Guastoni, H. Azizpour, P. Schlatter, and R. Vinuesa, Predictions of turbulent shear flows using deep neural networks, *Physical Review Fluids* **4**, 054603 (2019).
- [22] R. Wan, S. Mei, J. Wang, M. Liu, and F. Yang, Multivariate temporal convolutional network: A deep neural networks approach for multivariate time series forecasting, *Electronics* **8**, 876 (2019).
- [23] S. Bai, J. Z. Kolter, and V. Koltun, An empirical evaluation of generic convolutional and recurrent networks for sequence modeling (2018), [arXiv:1803.01271](https://arxiv.org/abs/1803.01271).
- [24] Z. Gan, C. Li, J. Zhou, and G. Tang, Temporal convolutional networks interval prediction model for wind speed forecasting, *Electric Power Systems Research* **191**, 106865 (2021).
- [25] P. Wu, F. Qiu, W. Feng, F. Fang, and C. Pain, A non-intrusive reduced order model with transformer neural network and its application, *Physics of Fluids* **34**, 115130 (2022).
- [26] A. Vaswani, N. Shazeer, N. Parmar, J. Uszkoreit, L. Jones, A. N. Gomez, L. Kaiser, and I. Polosukhin, Attention is all you need, in *Advances in Neural Information Processing Systems*, Vol. 30, edited by I. Guyon, U. V. Luxburg, S. Bengio, H. Wallach, R. Fergus, S. Vishwanathan, and R. Garnett (2017).
- [27] A. Gillioz, J. Casas, E. Mugellini, and O. A. Khaled, Overview of the transformer-based models for NLP tasks, in *2020 15th Conference on Computer Science and Information Systems (FedCSIS)* (2020) pp. 179–183.
- [28] K. Han, Y. Wang, H. Chen, X. Chen, J. Guo, Z. Liu, Y. Tang, A. Xiao, C. Xu, Y. Xu, Z. Yang, Y. Zhang, and D. Tao, A survey on vision transformer, *IEEE Transactions on Pattern Analysis and Machine Intelligence* **45**, 87 (2023).
- [29] M. Z. Yousif, M. Zhang, L. Yu, R. Vinuesa, and H. Lim, A transformer-based synthetic-inflow generator for spatially developing turbulent boundary layers, *Journal of Fluid Mechanics* **957**, A6 (2023).

- [30] N. Geneva and N. Zabaras, Transformers for modeling physical systems, *Neural Networks* **146**, 272 (2022).
- [31] A. Solera-Rico, C. Sanmiguel Vila, and M. e. a. Gómez-López, β -variational autoencoders and transformers for reduced-order modelling of fluid flows, *Nat Commun* **15**, 1361 (2024).
- [32] S. Cao, Choose a transformer: Fourier or Galerkin, in *Advances in Neural Information Processing Systems*, Vol. 34, edited by M. Ranzato, A. Beygelzimer, Y. Dauphin, P. Liang, and J. W. Vaughan (Curran Associates, Inc., 2021) pp. 24924–24940.
- [33] A. Katharopoulos, A. Vyas, N. Pappas, and F. Fleuret, Transformers are rnns: fast autoregressive transformers with linear attention, in *Proceedings of the 37th International Conference on Machine Learning*, ICML'20 (JMLR.org, 2020).
- [34] N. Kitaev, Lukasz Kaiser, and A. Levskaya, Reformer: The efficient transformer (2020), [arXiv:2001.04451](https://arxiv.org/abs/2001.04451).
- [35] S. Wang, B. Z. Li, M. Khabsa, H. Fang, and H. Ma, Linformer: Self-attention with linear complexity, *ArXiv abs/2006.04768* (2020).
- [36] T. Dao, Flashattention-2: Faster attention with better parallelism and work partitioning (2023), [arXiv:2307.08691](https://arxiv.org/abs/2307.08691).
- [37] L. Chierchia, Kolmogorov–arnold–moser (kam) theory, in *Encyclopedia of Complexity and Systems Science*, edited by R. A. Meyers (Springer New York, New York, NY, 2009) p. 5064–5091.
- [38] S. L. Brunton and J. N. Kutz, *Data-driven science and engineering: Machine learning, dynamical systems, and control* (Cambridge Univ.Press, 2022).
- [39] D. Bahdanau, K. Cho, and Y. Bengio, Neural machine translation by jointly learning to align and translate, arXiv preprint [arXiv:1409.0473](https://arxiv.org/abs/1409.0473) (2014).
- [40] J. Moehlis, H. Faisst, and B. Eckhardt, A low-dimensional model for turbulent shear flows, *New Journal of Physics* **6**, 56 (2004).
- [41] N. Satvat, F. Sarikurt, K. Johnson, I. Kolaja, M. Fratoni, B. Haugh, and E. Blandford, Neutronics, thermal-hydraulics, and multi-physics benchmark models for a generic pebble-bed fluoride-salt-cooled high temperature reactor (fhr), *Nuclear Engineering and Design* **384**, [10.1016/j.nucengdes.2021.111461](https://doi.org/10.1016/j.nucengdes.2021.111461) (2021).
- [42] E. N. Lorenz, Deterministic nonperiodic flow, *Journal of Atmospheric Sciences* **20**, 130 (1963).
- [43] H. Eivazi, L. Guastoni, P. Schlatter, H. Azizpour, and R. Vinuesa, Recurrent neural networks and koopman-based frameworks for temporal predictions in a low-order model of turbulence, *International Journal of Heat and Fluid Flow* **90**, 108816 (2021).
- [44] J. Pathak, Z. Lu, B. R. Hunt, M. Girvan, and E. Ott, Using machine learning to replicate chaotic attractors and calculate lyapunov exponents from data, *Chaos: An Interdisciplinary Journal of Nonlinear Science* **27** (2017).
- [45] Y. Wang, A. Solera-Rico, C. Sanmiguel Vila, and R. Vinuesa, Towards optimal β -variational autoencoders combined with transformers for reduced-order modelling of turbulent flows, *International Journal of Heat and Fluid Flow* **105**, 109254 (2024).
- [46] J. Wayland, C. Coupette, and B. Rieck, Mapping the multiverse of latent representations (2024), [arXiv:2402.01514 \[cs.LG\]](https://arxiv.org/abs/2402.01514).
- [47] G. Locatelli, M. Mancini, and N. Todeschini, Generation iv nuclear reactors: Current status and future prospects, *Energy Policy* **61**, 1503–1520 (2013).
- [48] A. L. Qualls, B. R. Betzler, N. R. Brown, J. J. Carbajo, M. S. Greenwood, R. Hale, T. J. Harrison, J. J. Powers, K. R. Robb, J. Terrell, A. J. Wysocki, J. C. Gehin, and A. Worrall, Preconceptual design of a fluoride high temperature salt-cooled engineering demonstration reactor: Motivation and overview, *Annals of Nuclear Energy* **107**, 144–155 (2017).
- [49] R. Hu, L. Zou, G. Hu, D. Nunez, T. Mui, and T. Fei, *SAM Theory Manual*, Technical Report ANL/NSE-17/4 Rev. 1 (Argonne National Laboratory, 2021).
- [50] J. Li, V. Seker, T. Downar, S. Kinast, N. Satvat, D. O’Grady, and R. Hu, Neutronics and thermal-hydraulics simulation of generic pebble-bed fluoride-salt-cooled high-temperature reactor (gfhr) (ANS - American Nuclear Society, 2022) p. 1812–1821, iNIS Reference Number: 54002322.
- [51] I. Mezić, Operator is the model (2023), [arXiv:2310.18516 \[math.DS\]](https://arxiv.org/abs/2310.18516).
- [52] K. J. Palmer, Shadowing lemma for flows, *Scholarpedia* **4**, 7918 (2009), revision #91761.
- [53] J. Thickstun, The transformer model in equations, johnthickstun.com (2020).
- [54] A. Paszke, S. Gross, S. Chintala, G. Chanan, E. Yang, Z. DeVito, Z. Lin, A. Desmaison, L. Antiga, and A. Lerer, Automatic differentiation in pytorch, in *NIPS 2017 Workshop on Autodiff*, Vol. 1 (2017) pp. 1–4.